Relaxation dynamics of the gel to liquid-crystalline transition of phosphatidylcholine bilayers

Effects of chainlength and vesicle size

William W. van Osdol, Michael L. Johnson, Qiang Ye, and Rodney L. Biltonen
Departments of Biochemistry and Pharmacology, University of Virginia School of Medicine, Charlottesville, Virginia 22908 USA

ABSTRACT The relaxation kinetics of the gel to liquid-crystalline transition of five phosphatidylcholine ($DC_{14}PC$ to $DC_{18}PC$) bilayer dispersions have been investigated using volume perturbation calorimetry, a steady-state technique which subjects a sample to sinusoidal changes in volume. Temperature and pressure responses to the volume perturbation are measured to monitor the relaxation to a new equilibrium position. The amplitude demodulation and phase shift of these observables are analyzed with respect to the perturbation frequency to yield relaxation times and amplitudes. In the limit of low perturbation frequency, the temperature and pressure responses are proportional to the equilibrium excess heat capacity and bulk modulus, respectively.

At all temperatures, the thermal response data are consistent with a single primary relaxation process of the lipid. The less accurate bulk modulus data exhibit two relaxation times, but it is not clear whether they reflect lipid processes or are characteristic of the instrument. The observed thermal relaxation behavior of all multilamellar vesicles are quantitatively similar. The relaxation times vary from ~50 ms to 4 s, with a pronounced maximum at a temperature just greater than T_m, the temperature of the excess heat capacity maximum. Large unilamellar vesicles also exhibit a single relaxation process, but without a pronounced maximum in the relaxation time. Their relaxation time is ~80 ms over most of the transition range.

INTRODUCTION

The phase behavior of model lipid bilayer systems has been the focus of extensive experimental and theoretical study. Particular attention has been paid to the transition between the gel and liquid-crystalline phases, which has been found to occur in natural membranes (Melchior and Steim, 1976). Many of the structural details of these two phases are now well understood (Luzzati and Tardieu, 1974; Cevc and Marsh, 1987), and a number of statistical mechanical models of the transition have been proposed (Nagle, 1980; Mouritsen, 1990 and references therein). The transition is readily produced thermotropically and occurs over a narrow, but finite, temperature range in which both the heat capacity at constant pressure and the isothermal elastic compliance display a sharp maximum (Albon and Sturtevant, 1978; Biltonen, 1990; Evans and Kwok, 1982). The heat capacity and isothermal elastic compliance are related to the mean-square amplitude of fluctuations in enthalpy and specific area, respectively. Thus, the amplitudes of these fluctuations are enhanced during the transition, and several studies suggest that they may be biologically relevant. For example, the passive permeability of bilayers to certain electrolytes and nonelectrolytes (Bangham et al., 1965; McElhaney et al., 1973), and the rate of activation of phospholipase A_2 using large unilamellar vesicles of saturated phosphotidylcholine as substrate (Lichtenberg et al., 1986) are found to be maximal near the midpoint of the transition. These equilibrium fluctuations are dynamic phenomena and an important aspect of their character is the time scales over which they occur and how various membrane components affect these times.

A number of kinetic studies utilizing transient and steady-state techniques have focused on the gel to liquid-crystalline transition. A short, critical review of some of this work can be found in van Osdol et al. (1989), and an exhaustive bibliography of kinetic studies of phase transitions in lipid systems is provided by Caffrey (1989). Because of the organizational complexity of lipid bilayers, the many physical changes involved in the transition, and the variety of techniques used to study the dynamics, a wide range of relaxation times from tens of nanoseconds to seconds has been observed. Although there is little quantitative agreement among the results from techniques capable of examining similar ranges of relaxation times (temperature jump: Tsong and Kanehisa, 1977; Genz and Holzwarth, 1986; pressure jump: Gruenewald et al., 1980; Elamrani and Blume, 1983), these studies do agree qualitatively in finding that relaxation times and amplitudes are maximal at the transition temperature, T_m, and decline as $(T - T_m)$ diverges from zero (see also Mitaku et al., 1983). An exception to this observation is the result obtained by Yager and Peticolas (1982), who used Raman spectroscopy to monitor the degree of order in

Dr. van Osdol's current address is Laboratory for Mathematical Biology, National Cancer Institute, National Institutes of Health, Bethesda, Maryland 20892.

the lipid acyl chains after a pressure jump. Time-resolved x-ray diffraction (Caffrey, 1985; Laggner et al., 1987; Cunningham et al., 1988) has also been employed to follow the progress of the transition produced by heating at a constant rate or cooling passively. In this technique, the observables are the diffraction patterns which characterize the gel and liquid-crystalline phases. At the highest heating rates, Caffrey (1985) found that no more than 1 s was required to drive a dispersion of dipalmitoyl phosphatidylcholine ($DC_{16}PC$) from the gel to the liquid-crystalline phase. Kreichbaum and coworkers (1990), also using x-ray diffraction with very fast infrared heating, observed that the transition was essentially complete within the time resolution of the measurement of ~1 ms.

In this article we describe the relaxation behavior of several phosphatidylcholine bilayer systems using steady-state volume perturbations to shift the transition equilibrium. Temperature and pressure were simultaneously monitored to observe the system response to the perturbation. The data have been analyzed in the frequency domain, yielding characteristic times for the approach to equilibrium. We present results for phosphatidylcholine lipids of varying chain length in multilamellar and large unilamellar vesicles.

MATERIALS AND METHODS

Volume perturbation calorimeter

A volume perturbation calorimeter, based on the design of Clegg and Maxfield (1976) as modified by Halvorson (1979), has been developed. A detailed description of the apparatus and the theory underlying its design can be found in van Osdol et al., 1989. Briefly, the instrument uses the voltage-dependent extension of a stack of piezoelectric crystals to produce small, adiabatic perturbations in the volume of a sample. This change in volume of the system causes pressure and temperature changes which shift the equilibrium point of the gel-liquid-crystalline transition. The T_m for $DC_{16}PC$ is linearly dependent on hydrostatic pressure, with a slope of 0.024 ± 0.003°C/atm (Mountcastle et al., 1978), as predicted by the Clausius-Clapeyron equation:

$$dT_m/dP = \Delta V/\Delta S = T_m\Delta V/\Delta H, \quad (1)$$

where ΔS, ΔV, and ΔH, are the molar changes in entropy, volume, and enthalpy, respectively. A shift in T_m induces a change in the fractional completion of the transition, which is monitored by temperature and pressure changes in the sample by means of a high-speed thermistor and pressure transducer.

Experiments are performed with all aspects of the volume perturbation calorimeter under computer control: synthesis of the voltage waveform which drives the crystal stack, data collection, and temperature control. Temperature and pressure data are collected with a 12-channel, simultaneous, direct-memory-access analogue-to-digital converter (model DT3388; Data Translation, Inc., Marlboro, MA). The signal-to-noise ratio of the instrument is improved by using signal averaging techniques. Temperature control of the sample is maintained by a programmable water bath (model RTE-9DD; Neslab Instruments, Inc., Portsmouth, NH). The set point of the water bath is programmed by the data acquisition computer via a 16-bit digital-to-analogue converter.

The instrument is capable of operating in both transient and stationary modes. All results reported herein were obtained with the instrument operating in the stationary mode, in which small oscillations in sample volume are produced by driving the crystal stack with a sinusoidal voltage over a selected frequency bandwidth. The voltage driving the crystal stack, and the sample temperature and pressure are measured over time, and their Fourier series are computed. From these series the two transfer functions characterizing the response of the system are formed: the ratio of the temperature to pressure changes and the ratio of the pressure to volume changes. These transfer functions characterize the "frequency dependent" heat capacity, $C_p(\omega)$, and bulk modulus (inverse of the isothermal compressibility), $B_T(\omega)$, respectively. Linear response theory is used to describe how the heat content and pressure of a system respond to a time-dependent volume change, and the fluctuation-dissipation theorem is then invoked to connect the transfer functions to the Fourier transform of the autocorrelation function of the fluctuations in enthalpy and volume, respectively (van Osdol et al., 1989). The application of linear response theory requires the perturbation to be small and that the time-dependent response is symmetrical. The typical pressure change of ±2 atm is equivalent to a temperature perturbation of ±0.048°C and the symmetry of the response was ascertained by the absence of even harmonics in the temperature response function.

The relaxation times for the system under steady-state perturbation are obtained from analysis of the amplitude demodulation and phase shift of the transfer functions as functions of the perturbation frequency. These relaxation times characterize some of the relaxation modes of the enthalpy and volume fluctuations; exactly which modes are being characterized depends on the relaxation mechanism and on the range of the perturbation frequency.

Vesicle preparation

Phosphatidylcholines were obtained as the chloroform solution from Avanti Polar Lipids, Inc. (Birmingham, AL) and were stored frozen until used. The purity of each lipid was checked by thin layer chromatography (TLC), using the solvent system $CHCl_3$, CH_3OH, NH_4OH, H_2O, 65:35:3:3 (vol/vol) (Kates, 1972). Iodine vapor was used to develop the plates. Each lipid was found to run as a single spot and was used without further purification.

To prepare a lipid for dispersion in aqueous medium, the chloroform solution was placed in a test tube and the solvent evaporated under a stream of nitrogen. Care was taken that the lipid thinly and evely coated the walls of the test tube. The lipid was then lyophilized for at least 12 h.

Multilamellar vesicles (MLV) were prepared as follows. A test tube containing thoroughly dried lipid was immersed in a water bath 10°–15°C > T_m. The aqueous medium was also heated to this temperature, and a sufficient amount added to the lipid to give the desired lipid concentration (usually 75 mM). This mixture was then vortexed in 5 s bursts every 5 min over a 30 min period. The dispersion was then slowly cooled through the transition range over the course of 30–45 min. Large unilamellar vesicles (LUV) of ~120 nm diameter were prepared from MLV by an extrusion method (Hope et al., 1985; and Mayer et al., 1986).

The aqueous medium used in all experiments was 50 mM TES, 50 mM KCl, 1 mM NaN_3, pH 7.4 (at the appropriate T_m). During the preparation of MLV of a particular lipid, sufficient sucrose was included in the medium to raise the solvent density to that of the vesicles at their T_m. This ensured that the vesicles did not separate from the bulk aqueous medium during the course of an experiment. 0.46 M sucrose was used for $DC_{14}PC$, 0.30 M for $DC_{15}PC$, 0.18 M for

$DC_{16}PC$, 0.12 M for $DC_{17}PC$, and 0.06 for $DC_{18}PC$ (Nagle and Wilkinson, 1978). The effect of sucrose on the relaxation behavior of MLV could not be determined directly because of vesicle separation if the sucrose concentration was not near that required to equalize the vesicle and solvent density at the T_m. However, it is unlikely that the relaxation behavior of all MLV preparations would fortuitously be essentially identical if sucrose had a dramatic effect on the kinetics of the transition. Furthermore, the relaxation behavior of LUV was found to be identical in the presence and absence of sucrose.

Before the kinetic experiment, the lipid dispersion was characterized by high-sensitivity heat-conduction differential scanning calorimetry (DSC) (Suurkuusk et al., 1976). Typically, the lipid was compared to a water reference at a scan rate of 10°C/h or slower. Analysis of the DSC data provided the thermodynamic information necessary to plan the course of the kinetic experiment: the temperature range and enthalpy change of the transition, and the shape of the excess heat capacity curve.

Kinetic experiment

The kinetic experiments were performed according to the following protocol. A lipid dispersion was loaded into the volume perturbation calorimeter and placed under a small static pressure (12–18 atm). The sample was then brought to thermal equilibrium at a succession of temperatures which covered the transition region. After thermal equilibration, the voltage, and pressure and temperature response data were collected in the frequency range of 0.01–150 Hz.

The voltage waveform used in all these experiments consisted of the first three components of a square wave: a fundamental sine wave, plus its third and fifth harmonics. The amplitude of the voltage waveform was sufficient to produce a relative change of $\sim \pm 10^{-4}$ in the sample volume. This corresponds to pressure oscillations of ±2 atm about the equilibrium pressure.

Data analysis

At each equilibrium temperature, the Fourier components of the signal-averaged voltage, pressure, and temperature response data were computed. Because the response of the system was assumed to be linear, only the sine and cosine terms of the fundamental, third and fifth harmonic frequencies were computed. The mean-square error in the Fourier representation was then calculated and used to assign a standard error to each Fourier component.

The components and their error estimates were transformed from analogue-to-digital converter units to physical units, and the representation was then changed from the sine and cosine series to the sine series involving amplitudes and phase angles. Each series (voltage, pressure, and temperature) consisted of a constant and three sine terms (one at the fundamental frequency and at the third and fifth harmonic), each of the latter having an amplitude and phase angle. The frequency-dependent heat capacity transfer function, $C_p(\omega)$, was then calculated by forming the ratios of the amplitudes, and the differences of the phase angles of the corresponding harmonics of the series for temperature and pressure. The same procedure using the series for pressure and voltage yielded the transfer function $B_T(\omega)$.

Before analysis, the transfer functions were normalized to account for the dynamic response characteristics of the volume perturbation calorimeter and contributions made by the aqueous medium. This was done by using data from volume perturbation experiments (at appropriate equilibrium temperatures, pressures, and frequencies) with water as the sample. The amplitudes of the transfer functions were computed for these data. At each frequency, the amplitudes of the transfer functions for the lipid dispersion were divided by the amplitudes of the transfer functions for the solvent. It was found that an instrument response correction of the phase angle data was unnecessary (van Osdol et al., 1989).

Using a nonlinear least-squares algorithm (Johnson and Frasier, 1985), the normalized amplitude data for each transfer function were then fit to

$$\{(\Sigma\, \alpha_i\omega\tau_i/[1 + (\omega\tau_i)^2])^2 + (\Sigma\, \alpha_i/[1 + (\omega\tau_i)^2])^2\}^{1/2}, \quad (2)$$

and the phase angle data were fit to

$$\tan^{-1}\{(\Sigma\, \alpha_i\omega\tau_i/[1 + (\omega\tau_i)^2])/(\Sigma\, \alpha_i/[1 + (\omega\tau_i)^2])\}, \quad (3)$$

where α_i and τ_i are the amplitude and relaxation time of the assumed ith independent relaxation process, respectively, and ω is the perturbation frequency.

RESULTS

Multilamellar vesicles

Experiments were conducted with five members of the homologous series of phosphatidylcholines having identical, fully saturated acyl chains from 14 carbons to 18 carbons in length. The results for $DC_{16}PC$ MLV are discussed in detail, because they are representative of the results obtained with the other homologues.

Fig. 1 is the heat capacity curve obtained by differential scanning calorimetry for a 75 mM dispersion of multilamellar vesicles of $DC_{16}PC$. The scan rate was 0.1°C/h, slow enough so that the heat transfer characteristics of instrument contributed negligibly to the observed signal. T_m, the temperature for maximal excess heat capacity, was 41.4°C, and the transition half-width at half-height was 0.076°C. The enthalpy change for the transition was estimated to be 8.4 kcal/mol.

The amplitude and uncorrected phase angle data of $C_p(\omega)$, and the amplitude data of $B_T(\omega)$, all at a scaled temperature of 41.4°C, are plotted as function of $\log_{10}$ of

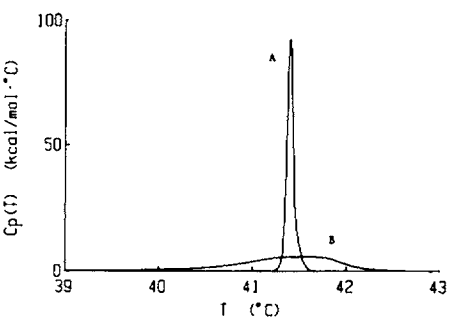

FIGURE 1 (*A*) The excess heat capacity of MLV of $DC_{16}PC$ plotted as a function of temperature. The scan rate was 0.1°C/h, slow enough so that any distortion due to the response time of the calorimeter was absent. The excess heat capacity was maximal at 41.4°C; the half-width at half maximum was 0.076°C. (*B*) The excess heat capacity of LUV of $DC_{16}PC$ as a function of temperature.

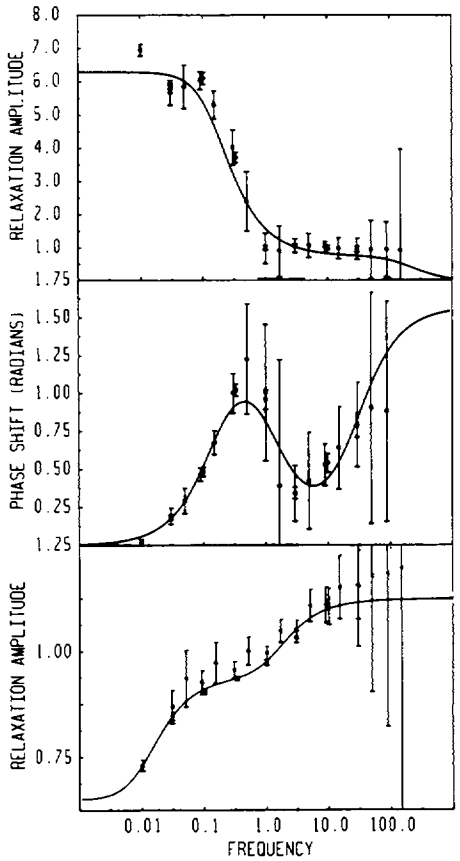

FIGURE 2 (*Upper*) Graph of the amplitude of $C_p(\omega)$, of 75 mM $DC_{16}PC$ MLV at T_m, as a function of $\log_{10}$ of the perturbation frequency. The ordinate is in units of the response due to water in this temperature range, 0.0029°C/atm. The solid line represents the best fit of the data to two relaxation processes, the faster one accounting for the baseline observed at higher frequencies and not pertinent to relaxation in the lipid itself. The standard errors in the data are indicated by the vertical lines. (*Middle*) Graph of the phase shift of $C_p(\omega)$, (in radians), no correction has been performed. The solid line is the best fit of the data to two relaxation processes, with the faster characterizing the high-frequency baseline. (*Lower*) The amplitude of $B_T(\omega)$. The units of the ordinate are the bulk modulus of water in this temperature range: 2×10^{-4} atm. The solid line is the best fit of the data to three relaxation processes, the fastest and slowest of which characterize aspects of the instrument itself. These results are similar to those reported in van Osdol et al. (1989).

the perturbation frequency in Fig. 2. The scaled temperature is defined as $T_s = T - 0.024P$, where P is the mean pressure for $DC_{16}PC$ MLV dispersion during an experiment, and 0.024 is equal to $(dT_m/dP)_s$ previously determined (Mountcastle et al., 1978). The phase angles for $B_T(\omega)$ were too small to allow them to be analyzed successfully. Error bars are included, and the solid lines represent the best fits of the data to the sums of relaxation terms in Eqs. 2 and 3. The amplitude and phase shift data of $C_p(\omega)$ are consistent with a single relaxation process, but the amplitude data of $B_T(\omega)$ suggest two relaxation processes.

Fig. 3 *a* shows the amplitude of $C_p(\omega)$, plotted as a function of the scaled temperature at four frequencies: 0.01, 0.1, 1, and 10 Hz. The ordinate is in units equal to the response obtained with only water in the sample cell at these temperatures, 2.9×10^{-3}°C/atm. At the lower frequencies these curves closely resemble the equilibrium excess heat capacity curve. They exhibit a half-width at half-height approximately twice that estimated from the equilibrium heat capacity curve, presumably due to the finite size of the perturbation. The scaled

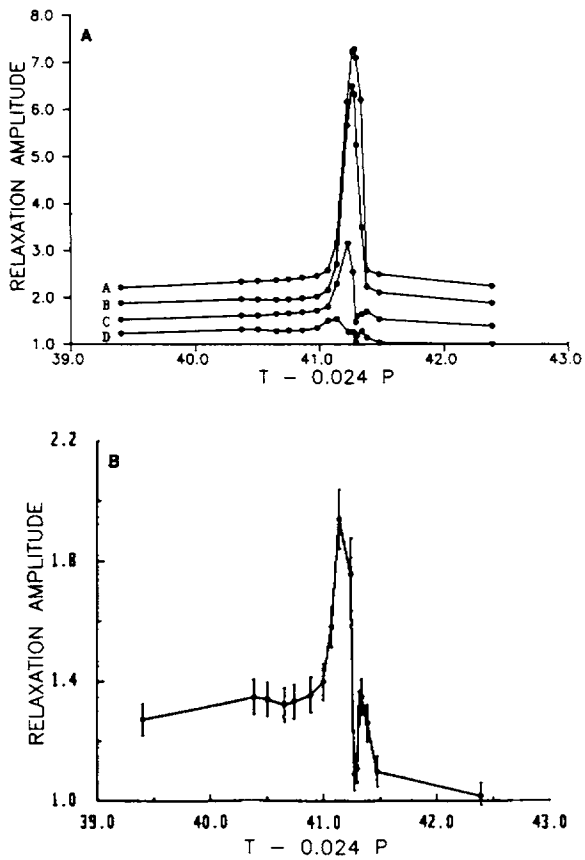

FIGURE 3 (*A*) The amplitude of the transfer function $C_p(\omega)$ of 75 mM $DC_{16}PC$ MLV, as a function of temperature, at four different volume perturbation frequencies: *A*, 0.01 Hz; *B*, 0.1 Hz; *C*, 1 Hz; and *D*, 10 Hz. Curves *A–C* have been displaced on the ordinate for clearer presentation. The abscissa is in degrees Celcius scaled by the equilibrium (static) pressure in the sample cell. The scaling factor is 0.024°C/atm. $C_p(\omega)$ has been normalized to account for instrumental and static contributions to the signal. The ordinate is in units of the water response at these temperatures: 0.0029°C/atm. Error bars have been omitted for clarity. (*B*) $C_p(\omega)$, for $\omega = 0.3$, plotted as a function of the scaled temperature. The vertical lines indicate the standard errors associated with the data. The splitting into major and minor peaks is pronounced and cannot be eliminated by consideration of the errors.

temperature of maximal response amplitude agrees with the temperature of maximal excess heat capacity, 41.4°C. The amplitudes decrease with increasing frequency, and fall to values close to unity outside the transition region. This reflects the fact that outside the transition region the heat capacity of the lipid dispersion is much like that of water. At perturbation frequencies >0.3 Hz, the thermal response amplitude splits into two peaks when plotted as a function of temperature (Fig. 3 *b*). This splitting was found for all five lipid species examined; it is not due to the baseline subtraction procedure, because it is also observed in the uncorrected amplitudes. This splitting is consistent with the observation that the relaxation process is slowest at the temperature where the trough is found, and faster at lower and higher temperatures.

In Table 1, the relaxation times obtained from the amplitude and phase angle data of $C_p(\omega)$ are listed with respect to the fractional completion of the transition, f. For a particular equilibrium temperature f was calculated by integrating the 0.01 Hz amplitude response curve (see Fig. 2) up to that temperature and normalizing that area by the total area under the curve. Because the amplitude response curve at this frequency was broader than the excess heat capacity curve obtained in the DSC experiment, the fractional degrees of completion are only approximately correct.

Both the amplitude and relaxation time are small at low values of f, and increase as f approaches the range 0.5–0.7, the neighborhood of the T_m. In this range, the amplitude was enhanced by about an order of magnitude over the minimum resolvable values. Above this rang of f, the relaxation amplitude again declined. However, the maximal relaxation time was found at $f \approx 0.8$ and was about two orders of magnitude longer than the shortest relaxation time resolvable. As f approached unity, the relaxation time decreased sharply. The relaxation times derived from the amplitude and phase angle data are identical within experimental error, in accordance with linear response theory.

Table 2 lists the relaxation amplitudes and times which characterize the two relaxation process observed for $B_T(\omega)$. The behavior of α_1 and τ_1 differed markedly from the case of $C_p(\omega)$. α_1 displayed a broad, low maximum about T_m, but τ_1 showed no particular development as a function of f. The errors associated with the relaxation amplitudes of B_T (ω) were such that relaxation times could not be estimated outside the range of f presented. We currently think that α_2 and τ_2 reflect heat exchange between the sample cell and the body of the calorimeter, and thus, do not reflect a relaxation mode of the bulk modulus of the sample (van Osdol et al., 1989). The pressure of the system should be more sensitive to heat exchange with the surrounding than is the temperature measured by the thermistor which is located near the center of the cell. It may be that α_1 and τ_1 also reflect an instrumental relaxation process; a relaxation process with a similar characteristic time was observed with water. The normalization procedure was designed to remove this contribution from the lipid data, implying that these relaxation amplitudes resolved from the lipid data were due to lipid. Nonetheless, the relaxation could be instrumental in origin.

In addition to the experiments just described, con-

TABLE 1 The relaxation amplitudes and times obtained from nonlinear least-squares analysis of $C_p(\omega)$ amplitudes and phase shift data for multilamellar vesicles of $DC_{16}PC$

f	Amplitude	Tau (s)
	$C_p(\omega)$ Amplitude	
0.06	1.09 (0.63, 1.53)	0.028 (0.013, 0.054)
0.33	4.43 (4.29, 4.58)	0.21 (0.19, 0.25)
0.46	5.84 (5.44, 6.24)	0.59 (0.45, 0.78)
0.61	5.32 (4.85, 5.80)	0.98 (0.74, 1.31)
0.73	4.91 (4.47, 5.36)	1.82 (1.31, 2.45)
0.82	3.92 (3.28, 4.54)	3.89 (2.63, 5.62)
0.91	0.61 (0.58, 0.64)	0.35 (0.32, 0.39)
	$C_p(\omega)$ Phase Shift	
0.33	6.8 (3.6, 11.1)	0.25 (0.21, 0.29)
0.46	6.7 (5.4, 8.3)	0.61 (0.55, 0.67)
0.61	8.3 (6.9, 10)	1.07 (0.97, 1.18)
0.73	5.6 (4.4, 7)	1.86 (1.59, 2.17)
0.82	2 (1.8, 2.3)	2.77 (2.48, 3.09)

The amplitude data were normalized to account for contributions due to the instrument and the aqueous medium as described in the text; the phase angle data were not. The fitted relaxation amplitudes (relative to water) and times are listed with respect to f, the fractional completion of the transition. The values in parentheses indicate the 1 SD confidence intervals.

TABLE 2 The relaxation amplitudes (relative to water) and times obtained from a nonlinear least-squares analysis of the $B_T(\omega)$ amplitude data from multilamellar vesicles of $DC_{16}PC$

f	$B_T(\omega)$ Amplitude			
	$Ampl_1$	Tau_1 (s)	$Ampl_2$	Tau_2 (s)
		s		*s*
0.33	0.073	0.20	0.13	10.2
0.46	0.12	0.14	0.22	12.0
0.61	0.14	0.15	0.25	11.5
0.73	0.14	0.20	0.42	20.9
0.82	0.09	0.55	0.25	14.8

The data were normalized to account for contributions due to the instrument and the aqueous medium as described in the text. Two relaxation processes were resolved, the slower of which we attribute to heat exchange between the sample and the body of the calorimeter. The fitted relaxation amplitudes and times are listed with respect to f, the fractional completion of the transition, and the values in parentheses indicate the 1 SD confidence intervals.

ducted at 75 mM $DC_{16}PC$, we performed experiments at 20, 30, 45, and 140 mM lipid. The relaxation times derived from these experiments were independent of lipid concentration and very close to those obtained at 75 mM lipid (van Osdol, 1988). Experiments performed with a volume perturbation sufficient to produce a ±1 atm pressure oscillation in the sample (half the usual amplitude) indicated that the relaxation times were also independent of the perturbation amplitude in this range (van Osdol, 1988).

Table 3 lists the relaxation times derived from the amplitude and phase data of $C_p(\omega)$ for MLV dispersions of $DC_{14}PC$, $DC_{15}PC$, $DC_{17}PC$, and $DC_{18}PC$. Comparing Tables 1 and 3, it is clear that all five homologues share the same relaxation behavior for $C_p(\omega)$. This is evident in Fig. 4 which shows the relaxation times derived from the amplitude data for $C_p(\omega)$, for all five homologues, plotted as functions of the fractional degree of completion. $B_T(\omega)$ results with these lipids were similar to those obtained with $DC_{16}PC$.

TABLE 3 Relaxation amplitudes (relative to water) and times (in seconds) obtained by nonlinear least-squares analysis of the amplitude and phase angle data for $C_p(\omega)$ for $DC_{14}PC$, $DC_{15}PC$, $DC_{17}PC$, and $DC_{18}PC$

	$C_p(\omega)$ ampl		$C_p(\omega)$ phase	
f	Ampl	Tau (s)	Ampl	Tau (s)
		$DC_{14}PC$		
0.40	5.89	0.19	3.32	0.21
0.50	6.77	0.49	4.31	0.50
0.67	6.86	0.62	5.14	0.74
0.80	6.84	2.04	2.54	1.64
0.93	1.20	0.21	0.44	0.44
		$DC_{15}PC$		
0.21	2.76	0.16	—	—
0.35	3.71	0.40	—	—
0.44	3.97	0.71	5.65	0.94
0.58	3.80	1.47	4.98	1.58
0.68	2.66	3.55	2.66	2.88
0.86	0.34	0.41	0.45	0.58
		$DC_{17}PC$		
0.30	1.69	0.04	2.7	0.03
0.50	3.75	0.10	4.1	0.12
0.65	4.62	0.29	5.1	0.30
0.73	4.20	0.76	5.2	0.86
0.83	2.16	2.40	1.6	2.84
0.95	0.57	0.25	—	—
		$DC_{18}PC$		
0.26	3.21	0.09	3.20	0.15
0.41	3.34	0.13	3.34	0.26
0.50	3.35	0.18	3.34	0.33
0.75	3.07	0.49	2.80	0.73
0.90	2.16	2.40	1.80	1.70
0.98	0.68	0.55	0.25	0.05

The lipid concentration was 75 mM. The amplitude data were normalized to account for contributions by the instrument and the aqueous medium as described in the text; the phase shift data were not. Confidence intervals have been omitted; they are essentially the same as those indicated in Table 1 for $DC_{16}PC$.

Large unilamellar vesicles

Large unilamellar vesicles of DPPC made by extrusion had a mean radius of 120 ± 40 nm, as characterized by quasielastic light scattering. The DSC scan of this dispersion, shown in Fig. 1, exhibited a broad transition beginning at ~38.5°C with a maximum at 41.0°C and ending at ~42°C. The scan was asymmetric and the transition half-width at half-height was 1.0°C. A slight shoulder at ~41.3°C was noted. We did not attempt to decompose these data into any constituent contributions although it is possible that the dispersion was composed of two distributions of vesicles, each behaving slightly differently thermodynamically.

Figs. 5 and 6 show the amplitudes of $C_p(\omega)$ and $B_T(\omega)$, respectively, as functions of the scaled temperature at perturbation frequencies of 0.01, 0.1, 1, and 10 Hz. The relaxation amplitudes as a function of temperature are similar in shape to the heat capacity function. At the lowest perturbation frequency the maximum amplitude is observed at a scaled temperature of 41.1 ± 0.1°C. The curves are skewed to the low temperature side of the transition and the half-widths at half-height are ~1.5°C, with maxima about half as great as those measured with

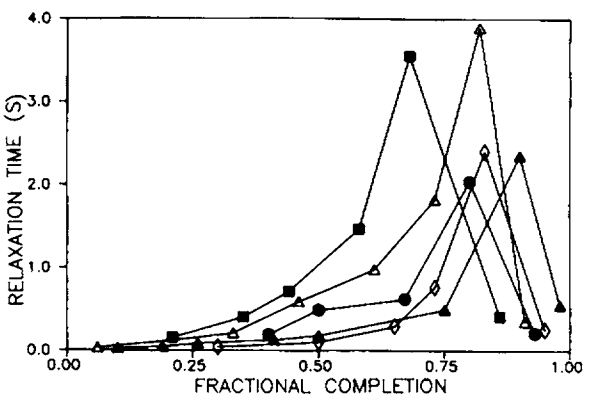

FIGURE 4 The characteristic time for relaxations in the amplitude of $C_p(\omega)$ in MLV of $DC_{14}PC$ (●); $DC_{15}PC$ (■); $DC_{16}PC$ (△); $DC_{17}PC$ (◇), and $DC_{18}PC$ (▲) as a function of the fractional degree of completion of the transitions. Error bars have been omitted for clarity. The relaxation times are listed in Tables 1 and 3.

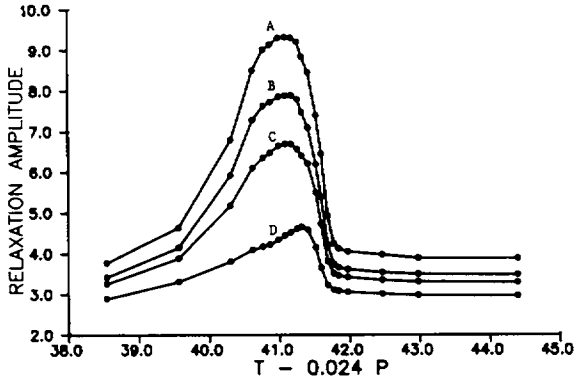

FIGURE 5 A plot of the amplitude of $C_p(\omega)$ for $DC_{16}PC$ LUV, as a function of scaled equilibrium temperature at four perturbation frequencies: *A*, 0.01 Hz; *B*, 0.1 Hz: *C*, 1 Hz, and *D*, 10 Hz. The ordinate is in units of 10^{-3}°C/atm. No correction has been performed to remove contributions of the aqueous medium or the instrument. Error bars have been omitted for clarity.

MLV of $DC_{16}PC$ at the same total lipid concentration. The splitting of the temperature profile of the $C_p(\omega)$ into two peaks, as observed in MLV at perturbation frequencies > 0.3 Hz, was not found with LUV.

Because the response amplitudes for LUV were rather low, the uncorrected $C_p(\omega)$ data were analyzed. Three relaxation times were found, two of which (4–6 ms, and 4–5 s) are characteristic of the instrument and the response contribution from the aqueous medium (van Osdol et al., 1989). If the data were normalized for the response of the instrument these relaxations would not be observed. The remaining relaxation time and amplitude reflect relaxation of the lipid, and are listed in Table 4. (It should be noted that amplitudes shown in Fig. 5 are the sum of this relaxation amplitude plus those which are associated with instrument responses.) Both parameters have a greater relative uncertainty than the corresponding quantities obtained from the MLV data. The relaxation amplitude displayed a broad, low maximum about the T_m, but the relaxation time was approximately constant at 80 ms over much of the transition region, declining at low and high fractional completion. This is quite different behavior from that observed with MLV. Previously, Mayorga et al. (1988) reported that the upper limit of the relaxation of $DC_{14}PC$ LUV was 80 ms near the T_m. This value was deduced from the frequency dependent response of a multifrequency calorimeter over the limited perturbation range of 0.04–1 Hz. They also reported a second process with a relaxation time of ~4s. whose amplitude was ~25% of that of the faster process. Our results obtained over a frequency range of 0.01–150 Hz confirm that the relaxation time of $DC_{16}PC$ LUV is 80 m. Similar results were obtained with $DC_{14}PC$ LUV.

Two relaxation times were resolved from the uncorrected $B_T(\omega)$ data for LUV, and the results are qualitatively and quantitatively the same as for MLV. Although the relaxation time resolved from the $C_p(\omega)$ data differed in the case of MLV and LUV, the relaxation times resolved from the $B_T(\omega)$ data for MLV and LUV were similar. This similarity leads us to suspect more strongly that these relaxation times reflect processes which have an instrumental origin.

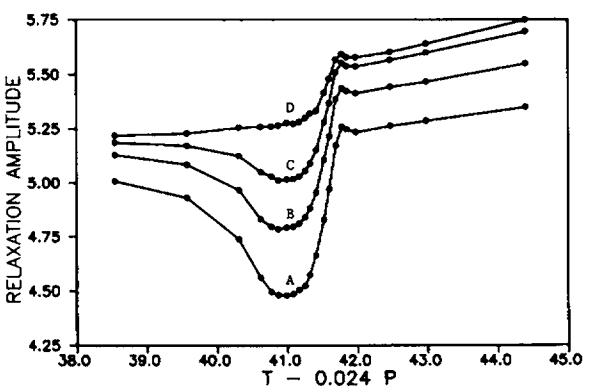

FIGURE 6 Plot of the amplitude of $B_T(\omega)$ for $DC_{16}PC$ LUV, as a function of scaled equilibrium temperature, at four perturbation frequencies: *A*, 0.01 Hz; *B*, 0.1 Hz; *C*, 1 Hz, and *D*, 10 Hz. No correction has been performed to remove contributions for the aqueous medium or the instrument. Error bars have been omitted for clarity.

TABLE 4 Relaxation amplitudes and times derived from nonlinear least-squares analysis of the uncorrected amplitude data from $C_p(\omega)$ obtained from $DC_{16}PC$ dispersed as large unilamellar vesicles

f	$C_p(\omega)$ Amplitude Amplitude (10^{-3} C/atm)	Tau (s)
0.22	1.7 (0.70, 3.21)	0.068 (0.036, 0.131)
0.36	2.46 (1.39, 3.5)	0.089 (0.048, 0.168)
0.46	2.69 (1.78, 3.58)	0.088 (0.054, 0.144)
0.52	2.81 (1.83, 3.78)	0.082 (0.051, 0.135)
0.62	2.9 (1.97, 4.0)	0.076 (0.046, 0.118)
0.69	2.78 (1.6, 3.93)	0.079 (0.045, 0.139)
0.75	2.59 (1.54, 3.6)	0.083 (0.049, 0.144)
0.80	2.24 (1.12, 3.34)	0.079 (0.042, 0.152)
0.85	2.03 (0.54, 3.47)	0.063 (0.028, 0.143)
0.89	2.03 (0.7, 4.05)	0.049 (0.018, 0.95)
0.92	1.77 (0.46, 3.83)	0.045 (0.014, 0.93)

The fitted quantities are listed with respect to *f*, the fractional completion of the transition, and the values in parentheses define the 1 SD confidence intervals.

DISCUSSION

We have used a stationary perturbation technique to examine the kinetics of the gel to liquid-crystalline phase transition in multilamellar vesicle dispersions of several phosphatidylcholines. The observables were the "frequency-dependent" heat capacity and bulk modulus. The frequency demodulation of the response amplitude, and phase shift of the heat capacity were consistent with a single primary relaxation mode, having a relaxation amplitude which was maximal at T_m, and a relaxation time maximal at slightly higher temperature (0.04–0.06°C). The characteristic times obtained from the amplitude and phase shift data agreed quite closely, in accordance with linear response theory.

The response amplitude of the bulk modulus displayed different relaxation characteristics: two relaxation modes, with relaxation times on the order of 200 ms and 15 s, respectively, were observed. We attribute the slower relaxation to heat transfer between the sample cell and the body of the calorimeter, but the faster relaxation has not been conclusively assigned to either an instrumental response or a process inherent to the lipid vesicles. *A priori*, one would expect a high correlation between temperature and pressure relaxation modes in vesicles because the excess heat capacity and excess compressibility have a common origin in the disordering of the lipid hydrocarbon chains. A conclusive test of this hypothesis by volume perturbation calorimetry will require further experimentation and, possibly, further development of the instrument.

The sum of the relaxation amplitudes, S, resulting from reequilibration of the lipid transition is related to the excess heat capacity of the system:

$$C_p \approx C_s S/(dT_m/dP - dT_s/cP - S), \quad (4)$$

where C_s is the heat capacity (per unit volume) of the lipid solution, exclusive of that due to the transition; dT_m/dP is the change in lipid melting temperature per atmosphere pressure perturbation; and dT_s/dP is the Joule-Thompson coefficient of system outside the transition range. It is to be noted that C_p is the value of the excess heat capacity per unit volume averaged over the range of the perturbation. For dispersions of $DC_{16}PC$ multilamellar vesicles $(dT_m/dP) = 0.024$°C/atm, $(dT_s/dP) = 0.003$°C/atm, and $C_s \approx 1$ cal/°c-ml. Thus, $C_p/C_s = S/(0.021 - S) = S'/(7 - S')$ where S is in units of °c/atm and S' is in units of the response of water to a 1 atm perturbation. Eq. 4 can be rearranged to yield

$$S' = 7C_p/(C_s + C_p), \quad (5)$$

which demonstrates that $S' \leq 7$, with the limit reached as the lipid concentration approaches infinity. The value of S' over the transition can be estimated from the equilibrium heat capacity results shown in Fig. 1 and compared to measured values as a function of lipid concentration. The results of this comparison at the transition temperature are shown in Table 5. S' (calculated) has a relatively large error because of the uncertainty in (dT_m/dP). Furthermore, S' (measured) will always be less than the true maximum value because of the finite size of the perturbation. Nevertheless, we can safely conclude that our measured relaxation amplitudes account for the majority, if not the entirety, of the lipid relaxations resulting from the pressure perturbations.

This result is to be contrasted with previous alternating current (ac) calorimetry experiments (Black and Dixon, 1980; Tenchov et al., 1989) in which low-frequency amplitudes were found to be much less than expected on the basis of equilibrium measurements. The differences between our results and those from ac calorimetry could be due to the tendency of the MLV to settle in the measuring cell during the experiment, thus, reducing the apparent concentrations in the dispersion. The ac calorimetry experiments may have suffered from this artifact because, apparently, no sucrose was used to keep the liposomes dispersed. The ac calorimetry experiments referred to also indicated that the apparent maximum in C_p was found at different temperatures depending upon whether the experiments were carried out in a heating or a cooling mode. Recent experiments in this laboratory (Ye, Q. unpublished data) indicate that the maximum amplitude occurs at the same scaled temperature (±0.03°C) in either mode. Thus, we have no evidence for hysteresis in the transition. Tenchov et al. (1989) have suggested that a metastable state devel-

TABLE 5 Comparison of the maximal theoretical and measured temperature response of different concentration of $DC_{16}PC$ MLV

[C]	S' (calculated)	S' (measured)
mM		
140	5.3-7.4	5.9
75	4.7-7.1	6.9
60	4.5-6.8	4.5
45	4.2-6.5	4.5
30	3.6-6.0	3.6

Comparison of the measured and maximal calculated amplitude of the temperature for different concentrations of $DC_{16}PC$ MLV. The range of S' (calculated) values has been obtained by assuming at one extreme that $dT_m/dP = 0.027$°C/atm and $C_L = 10^5$ cal/mol · deg, and at the other that $dT_m/dP = 0.21$°C/atm and $C_L = 5 \times 10^4$ cal/mol · deg. S' is given in units of the temperature response of water per atmosphere pressure change.

ops upon cooling $DC_{16}PC$ MLV through the transition, but Caffrey and co-workers (1990*b*) using x-ray diffraction have been unable to substantiate this. Caffrey et al. (1990*a*) also did not find evidence for hysteresis in either the gel to liquid-crystalline or liquid-crystalline to hexagonal phase transitions of phosphatidylethanolamine.

The general characteristics of the thermal relaxation behavior of the saturated phosphatidylcholines (C_{14}–C_{18}) MLV are identical. At low excitation frequencies, the temperature dependence of the relaxation amplitude mimics the equilibrium excess heat capacity, as predicted by theory. In all cases the primary relaxation time due to the lipid exhibits a maximum on the order of 2–4 s, which is 1–2 orders of magnitude longer than the relaxation time found at the high and low temperature edges of the transition. However, the maximal relaxation time is always observed at a temperature where the lipid is 60–90% in the liquid-crystalline state. This is shown clearly in Fig. 4. The exact significance of this observation is not certain, but it may be a reflection of the equilibrium topological distribution of gel and liquid-crystalline domains at different degrees of completion of the transition.

The physical process underlying the 2–4 s relaxation is not clear. It is also not known whether it is a process similar to or distinct from the faster relaxations occurring at slightly higher or lower temperatures. However, the relaxation of several seconds is only seen with multilamellar vesicles. In large unilamellar vesicles the maximum relaxation time is on the order of 80 ms. This suggests that bilayer–bilayer interactions may contribute to the slow relaxation. However, when the local anesthetic dibucaine (van Osdol, 1988) is included in multilamellar vesicle preparations the maximal relaxation time is reduced by a factor of 2–3 suggesting that the rate-limiting step is not solely determined by bilayer–bilayer interactions.

It is difficult to make a substantive comparison among the various reports on the dynamics of the gel to liquid-crystalline transition of bilayer lipid. The reasons for these difficulties include the broad variety of methods to induce the transition, the various methods to monitor the relaxation, and the magnitude of the perturbation to initiate the transition. Our studies with MLV are most similar to those of Tsong and Kanehisa (1977) who used small temperature jumps (0.2–0.3°C) to alter the equilibrium and used turbidity to monitor the relaxation process. These results were analyzed in terms of three time constants including one on the order of 10 s which may have been due to electroporation. The two faster relaxation times were maximal near the T_m. The amplitude of the slower of the two processes ($\tau \sim 2$ s for $DC_{14}PC$ and 0.4 s for $DC_{16}PC$ at the T_m) was a maximum near the T_m; the amplitude of the faster ($\tau \sim 35$–70 ms) was a minimum at the T_m.

Caffrey and co-workers (1990*b*) have used x-ray diffraction to monitor the $L_{\beta'}$ to L_α transition of $DC_{16}PC$ MLV as the sample was continuously heated. They always observed the development of the $P_{\beta'}$ form as an intermediate to formation of the L_α phase. It was also observed that the transit time for the transition was inversely proportional to the rate of heating. Kriechbaum et al. (1989) found that the transit time for the $L_{\beta'}$ to L_α transition of 1-stearoyl-2-oleoyl-*sn*-3-phosphotidylethanolamine was < 2 ms using rapid infrared heating. These results are not surprising because of the rapid heating rates used in these experiments and the fact that the transition took place under superheated conditions. At the highest heating rate (20–40°C/s) used by Caffrey et al. (1990*b*) to obtain transit times < 1 s, the initial observation of the L_α phase occurred ~ 4–8°C above the T_m.

Several other studies, using a fluorescence probe to monitor the transition, report relaxation times significantly shorter than our maximal value. These more rapid relaxations could be the result of the presence of the "contaminating" probe. As mentioned, anesthetics can cause an increase as the rate of the relaxation. Furthermore, the fluorescence relaxations may very likely be monitoring the local lipid relaxations in the vicinity of the probe rather than the global relaxations measured using the volume perturbation calorimeter. More work is required to clarify this situation.

The magnitude of the thermodynamic fluctuations of the lipid bilayer, as measured by the equilibrium heat capacity function, reflects the number and size of gel and liquid-crystalline clusters which coexist (Freire and Biltonen, 1978). However, C_p contains no information about the dynamic character of the various thermodynamic states. Because other processes in the membrane such as protein conformational change or diffusion of membrane components may be coupled to the lipid fluctuations, it is important to know the time scale of these fluctuations. For example, we have suggested that phospholipase A_2 activation on bilayer surfaces is dynamically coupled to the cooperative lipid structural fluctuations in or near the gel to liquid-crystalline transition region (Litchenberg et al., 1986). If this is true, then the intrinsic rate constant of activation, k_a, must be less than or equal to the reciprocal of the lipid relaxation time. This appears to be the case because k_a is on the order of 10^{-4}/s (Romero et al., 1987). Another relevant example is the diffusion of lipids within one monolayer, as measured by a fluorescence recovery after photobleaching (FRAP) experiment (Vaz et al., 1985). These authors have shown that the diffusion characteristics of the

probe whenever the chemically pure lipid exists even partially in the liquid-crystalline state are those observed for a totally liquid-crystalline bilayer (Vaz et al., 1990). Because rapid diffusion of the probe presumably only occurs within liquid clusters and because these clusters may be small relative to the bleaching area, this observation is most likely the result of the rapid fluctuations of cluster boundaries. Our results showing that the relaxation times of the lipid vary from <0.6 s at the theoretical percolation or connecting point of $f = 0.5$ for a hexagonal lattice (Stauffer, 1985) to $<3 \times 10^{-2}$ s at the transition onset are consistent with this interpretation.

It is thus obvious that interpretation of molecular events which might be coupled to the lipid gel to liquid-crystalline fluctuations requires knowledge of the kinetics of the transition. Studies of the type reported herein are being extended to include binary lipid systems and the effects of added constituents such as anesthetics and cholesterol on relaxation processes.

We thank Kim Thompson for his help in performing the differential scanning calorimetry experiments, and Denise Thompson for help in preparing the manuscript.

This work has been supported by grants from National Institutes of Health (GM-28928, GM37658 and DK38942) National Science Foundation (PCM-8300056 and DMB-8417175) and The Office of Naval Research (N0014-88-K-03260).

Received for publication 9 July 1990 and 26 November 1990.

REFERENCES

Albon, N., and J. M. Sturtevant. 1978. Nature of the gel to liquid crystal transition of synthetic phosphatidylcholines. *Proc. Natl. Acad. Sci. USA.* 75:2258–2260.

Bangham, A. D., M. M. Standish, and J. C. Watkins. 1965. Diffusion of univalent ions across the lamella of swollen phospholipids. *J. Mol. Biol.* 13:238–252.

Biltonen, R. L. 1990. A statistical thermodynamic view of cooperative structural change in phospholipid bilayer membranes: their potential role in biological function. *J. Chem. Thermodynamics.* 22:1–19.

Black, S. G., and G. S. Dixon. 1981. AC calorimetry of dimyristoylphosphatidylcholine multiplyers: hysteresis and annealing near the gel to liquid-crystal transition. *Biochemistry.* 20:6740.

Caffrey, M. 1985. Kinetics and the mechanism of the lamellar gel/lamellar liquid crystalline and lamellar/inverted hexagonal phase transition in phosphatidylethanolamine: a real time x-ray diffraction study using synchrotrom radiation. *Biochemistry.* 24:4826–4844.

Caffrey, M. 1989. The study of lipid phase transition kinetics by time-resolved x-ray diffraction. *Annu. Rev. Biophys. Biophys. Chem.* 18:159–186.

Caffrey, M., R. L. Magin, B. Hunnel, and J. Zhang. 1990*a*. Kinetics of the lamellar and hexagonal phase transition in phosphatidylethanolamine: a time-resolved x-ray diffraction study using a microwave-induced temperature jump. *Biophys. J.* 58:21–29.

Caffrey, M., G. Fanger, R. L. Magin, and J. Zhang. 1990*b*. Kinetics of the premelting ($L_{\beta'}$–$P_{\beta'}$) and main transition in hydrated dipalmitoylphosphatidylcholine. *Biophys. J.* 58:677–686.

Cevc, O., and D. Marsh. 1987. Phospholipid Bilayers: Physical Principles and Models. John Wiley & Sons, Inc., New York. 425 pp.

Clegg, R. M., and B. W. Maxfield. 1976. Chemical kinetics studies by a new small-pressure perturbation method. *Rev. Sci. Instrum.* 47:1383–1393.

Cunningham, B. A., W. Tamura-Lis, L. J. Lis, and P. J. Quinn. 1988. Time-resolved x-ray diffraction measurement of phosphatidylcholine-phosphatidylethanalamine mixture: effect of phosphatidylethanolamine acyl-chain length. *J. Colloid Interface Sci.* 121:193–197.

Elamrani, K., and A. Blume. 1983. Phase transition kinetics of phosphatidic acid bilayers. A pressure-jump relaxation study. *Biochemistry.* 22:3305–3311.

Evans, E., and R. Kwok. 1982. Mechanical calorimetry of large dimyristoylphosphotidylcholine vesicles in the phase transition region. *Biochemistry.* 21:4874–4879.

Freire, E., and R. L. Biltonen. 1978. Estimation of molecular averages and equilibrium fluctuations in lipid bilayer systems from the excess heat capacity function. *Biochem. Biophys. Acta.* 514:54–68.

Genz, A., and J. F. Holzwarth. 1986. Dynamic fluorescence measurements on the main phase transition of dipalmytoylphosphatidylchoine vesicles. *Eur. Biophys. J.* 13:323–330.

Gruenewald, B., A. Blume, and F. Watanabe. 1980. Kinetics investigations on the phase transition of phospholipid bilayers. *Biochim. Biophys. Acta.* 597:41–52.

Halvorson, H. 1979. Relaxation kinetics of glutamate dehydrogenase self-association by pressure perturbtion. *Biochemistry.* 18:2480–2487.

Hope, M. J., M. B. Bally, G. Webb, and P. R. Cullis. 1985. Production of large unilamellar vesicles by a rapid extrusion procedure. Characterization of size distribution trapped volume and ability to maintain a membrane potential. *Biochim. Biophys. Acta.* 812:55–65.

Johnson, M. L., and S. G. Frasier. 1985. Nonlinear least-square analysis. *Methods. Enzyme.* 117:301–342.

Kates, M. 1972. Techniques of Lipidology. North-Holland Publishing Co., Amsterdam.

Kriechbaum, M., G. Rapp, J. Hendrix, and P. Laggner. 1989. Millisecond time-resolved x-ray diffraction on liquid-crystalline phase transitions using infrared laster T-jump techniques and synchrotron radiation. *Rev. Sci. Instrum.* 60:2541–2544.

Laggner, P., K. Lohner, and K. Muller. 1987. X-Ray cinematography of phospholipid phase transitions with synchrotron radiation. *Mol. Cryst. Liq. Cryst.* 151:373–388.

Lichtenberg, D., G. R. Romero, M. Menashe, and R. L. Biltonen. 1986. Hydrolysis of dipalmitoylphosphatidylcholine large unilamellar vesicles by porcine pancreatic phospholipase A_2. *J. Biol. Chem.* 261:5334–5440.

Luzzati, V., and A. Tardieu. 1974. Lipid phases: structure and structural transitions. *Ann. Rev. Phys. Chem.* 25:79–94.

Mayer, L. D., M. J. Hope and P. R. Cullis. 1986. Vesicles of variable sizes produced by a rapid extrusion procedure. *Biochim. Biophys. Acta.* 858:161–168.

Mayorga, O. L., W. W. van Osdol, and E. Freire. 1988. Calorimetrically determined dynamics of complex unfolding transitions in proteins. *Proc. Natl. Acad. Sci. USA.* 85:9514–9518.

McElhaney, R. N., J. De Gier, and E. C. M. van der Naut-Kok. 1973. The effect of alterations in fatty acid composition and cholesterol content on the non-electrolyte permeability of *A laidlawii* cells and derived liposomes. *Biochim. Biophys. Acta.* 298:500–512.

Melchior, D. L., and J. M. Steim. 1976. Thermotropic transitions in biomembranes. *Annu. Rev. Biophys. Bioeng.* 5:205–238.

Mitaku, S., T. Jippo, and R. Kataoka. 1983. Thermodynamic properties of the lipid bilayer transition pseudocrotical phenomena. *Biophys. J.* 42:137–175.

Mountcastle, D. B., R. L. Biltonen, and M. J. Halsey. 1978. Effect of anesthetics and pressure on the thermotropic behavior of multilamellar dipalmitoylphosphatidylcholine liposomes. *Proc. Natl. Acad. Sci. USA.* 75:4906–4910.

Mouritsen, O. G. 1991. Computer simulations of cooperative phenomena in lipid membranes. *In* Molecular Description of Biological Membrane Components by Computer-Aided Conformational Analysis. Vol. I. R. Brusseur, editor. CRC Press, Boca Raton, FL. In press.

Nagle, J. F. 1980. Theory of the main lipid bilayer phase transition. *Annu. Rev. Phys. Chem.* 31:157–195.

Nagle, J. F., and D. A. Wilkinson, 1978. Lecithin bilayers: density measurements and molecular interactions. *Biophys. J.* 23:159–175.

Romero, G., K. K. Thompson, and R. L. Biltonen. 1987. The activation of porcine pancreatic phospholipase A_2 by dipalmitoyl-phosphatidylcholine large unilamellar vesicles. *J. Biol. Chem.* 262:13476–13482.

Stauffer, D. 1985. Introduction to Percolation Theory. Taylor, Taylor and Frances, London. 121 pp.

Suurkuusk, J., B. Lentz, Y. Barenholz, R. L. Biltonen, and T. E. Thompson. 1976. A calorimetric and fluorescent probe study of the gel-liquid crystalline phase transition in small single-lamellar dipalmitoylphosphatidylcholine vesicles. *Biochemistry.* 15:1343.

Tenchov, B. G., H. Yao, and I. Hatta. 1989. Time-resolved x-ray diffraction and calorimetric studies at low scan rates. *Biophys. J.* 56:757–768.

Tsong, T. Y., and M. I. Kanehisa. 1977. Relaxation phenomena in aqueous dispersions of synthetic lecithins. *Biochemistry.* 16:2674–2680.

van Osdol, W. W. 1988. Kinetics of the main phase transition in phospholipid vesicles. Ph.D. thesis. University of Virginia, Charlottesville, VA. 359 pp.

van Osdol, W. W., R. L. Biltonen, and M. L. Johnson. 1989. Measuring the kinetics of membrane phase transitions. *J. Biochem. Biophys. Methods.* 20:1–46.

Vaz, W. L. C., R. M. Clegg, and D. Hallmann. 1985. Translational diffusion of lipids in liquid crystalline phase phosphatidylcholine multibilayers. A comparison of experiment with theory. *Biochemistry.* 24:871–786.

Vaz, W. C. L., E. C. C. Melo, and T. E. Thompson. 1990. Fluid phase connectivity in an isomorphous, two component, two phase phosphatidylcholine bilayer. *Biophys. J.* 58:237–275.

Yager, P., and W. L. Peticolas. 1982. The kinetics of the main phase transition of aqueous dispersions of phospholipids induced by pressure jump and monitored by Raman spetroscopy. *Biochim. Biophys. Acta.* 688:775.